

ORIGINAL ARTICLE

Response of *Prochlorococcus* to varying CO₂:O₂ ratios

Sarah C Bagby^{1,3} and Sallie W Chisholm^{1,2}

¹Department of Biology, Massachusetts Institute of Technology, Cambridge, MA, USA and ²Department of Civil and Environmental Engineering, Massachusetts Institute of Technology, Cambridge, MA, USA

Carbon fixation has a central role in determining cellular redox poise, increasingly understood to be a key parameter in cyanobacterial physiology. In the cyanobacterium *Prochlorococcus*—the most abundant phototroph in the oligotrophic oceans—the carbon-concentrating mechanism is reduced to the bare essentials. Given the ability of *Prochlorococcus* populations to grow under a wide range of oxygen concentrations in the ocean, we wondered how carbon and oxygen physiology intersect in this minimal phototroph. Thus, we examined how CO₂:O₂ gas balance influenced growth and chlorophyll fluorescence in *Prochlorococcus* strain MED4. Under O₂ limitation, per-cell chlorophyll fluorescence fell at all CO₂ levels, but still permitted substantial growth at moderate and high CO₂. Under CO₂ limitation, we observed little growth at any O₂ level, although per-cell chlorophyll fluorescence fell less sharply when O₂ was available. We explored this pattern further by monitoring genome-wide transcription in cells shocked with acute limitation of CO₂, O₂ or both. O₂ limitation produced much smaller transcriptional changes than the broad suppression seen under CO₂ limitation and CO₂/O₂ co-limitation. Strikingly, both CO₂ limitation conditions initially evoked a transcriptional response that resembled the pattern previously seen in high-light stress, but at later timepoints we observed O₂-dependent recovery of photosynthesis-related transcripts. These results suggest that oxygen has a protective role in *Prochlorococcus* when carbon fixation is not a sufficient sink for light energy.

The ISME Journal (2015) 9, 2232–2245; doi:10.1038/ismej.2015.36; published online 7 April 2015

Introduction

The marine picophytoplankter *Prochlorococcus* is the most numerous oxygenic marine phototroph and has the smallest genome among them (Partensky *et al.*, 1999; Dufresne *et al.*, 2003). It maintains access to a very large pan-genome via horizontal gene transfer, with hotspots in genomic islands, some of which contain genes that clearly have a role in niche differentiation (Coleman *et al.*, 2006; Kettler *et al.*, 2007; Scanlan *et al.*, 2009). Its genomic diversity has allowed *Prochlorococcus* to thrive over a broad range of environmental conditions, with distinct lineages adapted to different light levels, temperatures, and nitrogen, phosphorus, oxygen, and iron availabilities (Moore *et al.*, 1995, 2002; Moore and Chisholm, 1999; Goericke *et al.*, 2000; Johnson *et al.*, 2006; Coleman and Chisholm, 2007; Kettler *et al.*, 2007; Lavin *et al.*, 2010; Malmstrom *et al.*, 2013). One constant across ecotypes is their relative fitness in oligotrophic waters (Partensky *et al.*, 1999; Dinsdale *et al.*, 2008), promoted by traits like high surface-to-

volume ratio and low phosphorus demand (Dufresne *et al.*, 2003; Van Mooy *et al.*, 2006, 2009). In these waters, *Prochlorococcus* can account for as much as half of net primary production at a given location (Vaulot *et al.*, 1995).

In oxygenic phototrophs, intracellular oxygen can reduce the efficiency of carbon fixation, because the enzyme Rubisco can catalyze the reaction of ribulose-1,5-bisphosphate with either CO₂ or O₂ (Bowes *et al.*, 1971). Carboxylation leads to the Calvin cycle; the energetically wasteful oxygenation reaction typically leads to photorespiration to clear the cytotoxic product 2-phosphoglycolate from the cell. The cyanobacterial carbon-concentrating mechanism is thought to promote carboxylation by accumulating CO₂ and sequestering Rubisco in O₂-impermeable carboxysomes (Price *et al.*, 2008), yet, in light, some cyanobacteria may photorespire almost constantly (Eisenhut *et al.*, 2008). Recent work suggests that the *Prochlorococcus* carbon-concentrating mechanism, although minimal, is highly efficient (Hopkinson *et al.*, 2014), compensating for the comparatively weak CO₂ affinity of *Prochlorococcus* Rubisco ($K_M \sim 260\text{--}750\text{ }\mu\text{M}$) (Scott *et al.*, 2007; Roberts *et al.*, 2012; Hopkinson *et al.*, 2014).

Carbon dioxide and oxygen are also linked in cyanobacteria by cellular redox poise. The health of the photosynthetic electron transport chain depends on the dynamic balance between oxidized and

Correspondence: SW Chisholm or SC Bagby, Department of Civil and Environmental Engineering, Massachusetts Institute of Technology, 15 Vassar Street, Cambridge, MA 02139, USA.

E-mail: bagby@geol.ucsb.edu or chisholm@mit.edu

³Current address: Marine Science Institute, Webb Hall, University of California, Santa Barbara, CA 93106, USA.

Received 14 April 2014; revised 6 February 2015; accepted 12 February 2015; published online 7 April 2015

reduced cofactors. Increasingly, that balance appears to feed into cellular signaling in many cyanobacteria, contributing not just to control of photosynthesis-related gene expression but also to systems from the circadian clock to phototaxis (Li and Sherman, 2000; Wakabayashi *et al.*, 2011; Kim *et al.*, 2012); it is not known whether *Prochlorococcus*, which has only a partial circadian clock (Holtzendorff *et al.*, 2008; Axmann *et al.*, 2009), makes use of redox poise as a signal. Redox poise can be threatened by factors at both ends of the electron transport chain: either an excess of arriving photons or an inability to siphon off sufficient reducing equivalents through carbon fixation can create what amounts to an impedance mismatch. In such cases, absent other photoprotective strategies, excess electrons can flow to molecular oxygen to produce damaging reactive oxygen species (Niyogi, 1999). Remarkably, in the course of genome reduction, *Prochlorococcus* appears to have ‘outsourced’ reactive oxygen species decontamination to its neighboring heterotrophic bacteria (Morris *et al.*, 2011, 2012) and to have minimized its protective strategies (Mella-Flores *et al.*, 2012), likely limiting its ability to handle acute changes in redox poise.

To explore the relationships between oxygen and carbon dioxide physiology in *Prochlorococcus*, we first tracked the growth and fluorescence of the high-light-adapted *Prochlorococcus* strain MED4 under CO₂ and O₂ levels ranging from atmospheric to near-zero, with CO₂:O₂ ratios ranging from ~1:5250 to >4:1 (ambient: ~1:550). We then performed whole-genome transcriptional profiling of the MED4 response to acute CO₂ and O₂ limitation over a 24-h time course. Although *Prochlorococcus* would not encounter absolute CO₂ limitation at the severe levels examined in this study, midday light intensities in tropical surface waters should be well above saturating cellular CO₂ fixation capacity (Hopkinson *et al.*, 2014), making a steep imbalance between photon flux and CO₂ fixation a regular occurrence. Previous studies have exposed *Prochlorococcus* to high-light shock and to high-peak irradiances in a day:night cycle (Steglich *et al.*, 2006; Zinser *et al.*, 2009; Mella-Flores *et al.*, 2012). The experiments reported here provide an opportunity to examine how *Prochlorococcus* responds when low CO₂ rather than high light causes a photosynthetic impedance mismatch, and how O₂ availability conditions this response.

Materials and methods

Growth experiment

Axenic *Prochlorococcus* MED4 was grown in Sargasso seawater-based Pro99 medium (Moore *et al.*, 2007) amended with 20-mm Na-HEPES pH 8.1. The addition of HEPES at this concentration did not affect growth rate (data not shown). Standing (non-sparged) cultures were maintained in 25-mm glass

tubes at 21 °C with continuous illumination at ~60 μmol photons m⁻² s⁻¹ for >30 generations before inoculation of experimental cultures. After inoculation, tubes were capped loosely and allowed to grow without bubbling for ~24 h (Shi and Xu, 2009). Tubes were then sampled, fitted with sterile cap-and-frit assemblies, and connected to gas lines. Parallel standing controls were left with their original caps. Gas mixtures were prepared and certified by Airgas. Gases were bubbled through Milli-Q water, then passed through a needle valve, a 0.2-μm filter, and, in the culture tube, a fritted glass tube (porosity C, Ace Glass, Vineland, NJ, USA). Sparging rates were maintained as steadily as possible at ~2 ml min⁻¹ given the limitations of standard gas-cylinder regulators.

Cultures were sampled daily by withdrawing 0.3 ml with a sterile transfer pipet. Experimental cultures were immediately resealed. Samples were protected from light and rapidly subsampled for bulk fluorescence measurements (data not shown) and flow cytometry. For flow cytometry, 10- or 100-μl samples were diluted to 1 ml with filtered seawater. Glutaraldehyde (5 μl, 25%) was added and samples were mixed, then incubated under foil for ~10 min. Fixed samples were flash-frozen in liquid nitrogen. Cells were counted using the blue (488 nm) laser on an Influx flow cytometer (Cytopeia, Seattle, WA, USA) with a 2-μm fluorescent bead standard. Quantification of flow cytometric results was performed in R (v. 2.12.0) (R Development Core Team, 2010) using the package curvHDR (v. 1.0-3) (Naumann *et al.*, 2010).

Transcriptional profiling

Axenic *Prochlorococcus* MED4 cultures were grown as described above at ~60 μmol photons m⁻² s⁻¹ and 21 °C for >30 generations before the shock experiment. Three parallel 1.2-l cultures were then inoculated and grown to mid-log phase in clear 2-l bottles sparged with air at ~10 ml min⁻¹. At t = -24-h, 400-ml fresh medium was transferred to each of 12 clear 500-ml bottles for pre-equilibration with the experimental gases. Gases (Airgas, Cambridge, MA, USA) were 360 p.p.m. CO₂ + <0.001% O₂ (balance N₂) for -O₂ shock; 40 p.p.m. CO₂ + <0.001% O₂ (balance N₂) for -CO₂/ -O₂ shock; and 40 p.p.m. CO₂ + 21% O₂ (balance N₂) for -CO₂ shock. Three bottles were sparged vigorously with each experimental gas, and three control bottles with air, for 24 h.

To start the experiment, each mid-log-phase 1.2-l culture was split into six and harvested by pelleting in sterile acid-washed 250-ml centrifuge bottles in a JA-14 rotor, spinning at 8000 r.p.m. for 10 min. Supernatants were immediately poured off and each pellet resuspended in 3-ml fresh medium. Cell suspensions were pooled and split evenly among four 500-ml bottles, each pre-equilibrated with a different gas. Bottles were swirled to mix, 21-ml

samples were immediately ($t=0$) withdrawn into 30-ml centrifuge tubes, and sparging continued. A 1-ml subsample was immediately removed from each sample for bulk fluorescence and flow cytometry and protected from light; these subsamples were processed as described above. Meanwhile, the remaining 20 ml of each sample was pelleted by spinning at 12 500 r.p.m. and 4°C for 10 min in a JA-25.50 rotor. Supernatants were immediately discarded and each pellet resuspended in 500-μl resuspension buffer (200 mM sucrose, 10 mM NaOAc pH 5.2, 5 mM EDTA). Cell suspensions were transferred to 1.5-ml tubes and flash-frozen in liquid nitrogen. Sampling for each timepoint was completed within 20 min (from withdrawal of samples to flash freezing). Samples were taken at $t=0$, 70 min, 3 h, 6 h, 9 h, 12 h, 18 h and 24 h.

For RNA extraction, cell suspensions were thawed in small batches and processed with the Mini RNA Isolation II kit (Zymo Research, Irvine, CA, USA). The manufacturer's protocol was followed except that cell lysis was allowed to continue for 20 min on ice. DNA was removed by treating 1 μg total nucleic acids with 2-μl Turbo DNasefree (Ambion, Foster City, CA, USA) in a 50-μl reaction for 1 h, followed by DNase inactivation according to the manufacturer's protocol. RNA was concentrated by ethanol precipitation and yields were quantified with Ribogreen (Molecular Probes, Carlsbad, CA, USA). RNA amplification (using the MessageAmp II—Bacteria kit (Ambion) with 200 ng input), labeling, and hybridization to the custom Affymetrix microarray MD4-9313 (Santa Clara, CA, USA) were performed by the MIT BioMicro Center (Cambridge, MA, USA). Amplification, labeling, and hybridization were performed for two biological replicates at timepoints $t=0$, 70 min, 6 h, 12 h and 24 h.

Microarray data analysis was performed in R. Chip images were processed using the package Harshlight (Suárez-Fariñas *et al.*, 2005) before RMA normalization with the package affy (Bolstad *et al.*, 2003). Microarray data were deposited in the GEO database with accession number GSE65684. Genes showing significant differential expression were identified by Bayesian time-series analysis using the package betr (Aryee *et al.*, 2009), controlling for false positives at $\alpha=0.02$ and setting the threshold for significance at $P(\text{differential expression})>0.98$ (that is, $P(\text{null})<0.02$). Clustering analysis of significantly differentially expressed genes was performed using the fuzzy c-means package Mfuzz (Futschik and Carlisle, 2005) with four cluster centers and 'fuzziness' parameter $m=1.1$.

Gene functional categorizations are as annotated in CyanoBase (<http://genome.kazusa.or.jp/cyanobase/>) as of May 2009, except where updated gene annotation or comparison with KEGG pathways prompted manual reassignment. These exceptions are marked with asterisks in Supplementary Table S1, which gives both the original and reassigned gene categories.

Results and Discussion

Growth rates under different steady-state CO₂ and O₂ regimes

We first asked how growth is affected by CO₂ and O₂ availability by sparging cultures of *Prochlorococcus* MED4 with different gas mixtures. Three CO₂ concentrations (high, 0.036% (~atmospheric); moderate, 0.018%; and low, 0.004%) and three O₂ concentrations (high, 21% (atmospheric); moderate, 10%; and low, <0.001%) were examined in combination to provide nine growth conditions. We expected that, under moderate CO₂ limitation, competition between Rubisco's carbon fixation and oxygenation reactions would cause a greater reduction in growth rate at high O₂ than at moderate or low O₂, whereas severe CO₂ limitation would inhibit growth at any O₂ level. We used flow cytometry to measure cell counts and per-cell chlorophyll fluorescence, a proxy for cellular chlorophyll concentration (DuRand *et al.*, 2002).

Notably, growth and per-cell chlorophyll fluorescence of MED4 sparged with any combination of moderate and high CO₂ and O₂ was nearly indistinguishable from growth of parallel controls grown under lab air without sparging (Figure 1). By contrast, cultures grown at low O₂ and either moderate or high CO₂ began to show slower growth within 2 days, and approached stationary phase at lower cell densities. That is, far from releasing cells from photorespiratory pressure, suboxic conditions appeared to disrupt *Prochlorococcus* MED4 growth. With sufficient CO₂ for continuous carbon fixation, cells grown under constant light should produce a steady stream of O₂ at photosystem II (PSII). That exogenous O₂ limitation nonetheless limited growth suggests that the photosynthetic O₂ supply is insufficient to meet some cellular need, perhaps because of rapid diffusive loss to the suboxic medium.

Low CO₂ severely limited growth at all O₂ levels, with little or no cell division observed at $t>1$ day (Figure 1a). Yet flow cytometry revealed O₂-dependent differences in chlorophyll fluorescence per cell among the low-CO₂ conditions, with a sharper drop under low O₂ than high or moderate O₂ (Figure 1b). Interestingly, in contrast to the pattern for growth, chlorophyll fluorescence per cell appeared to be more strongly influenced by low O₂ than low CO₂, as low O₂ caused a similarly steep decline at all CO₂ levels. These results suggest an indispensable role for O₂ under the growth conditions studied. We sought to investigate this role and its connection to CO₂ levels further by studying the response at the transcriptional level.

Global transcriptional responses to acute changes in CO₂ and O₂ supply

For the transcription experiment, we focused on the first 24 h after cultures were split four ways for transfer to air-sparged medium and the growth

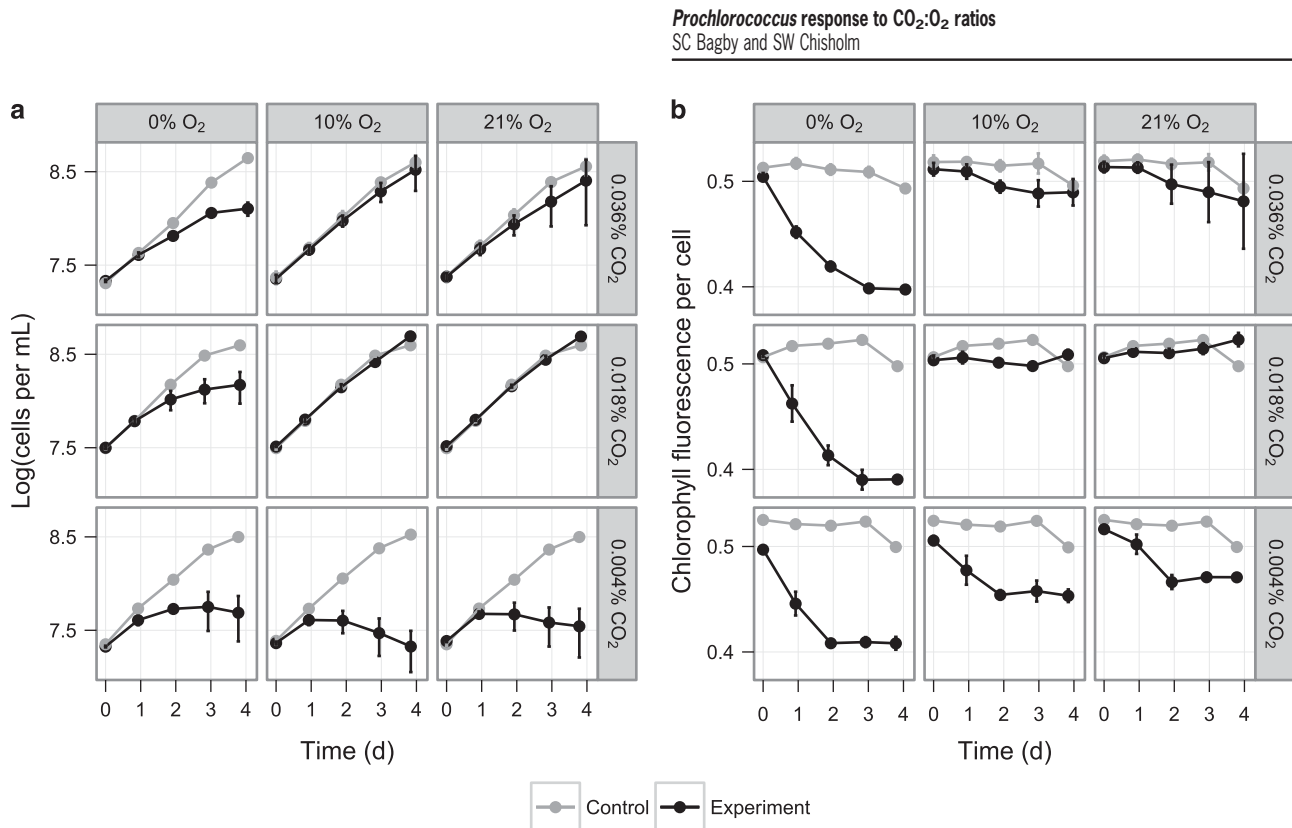
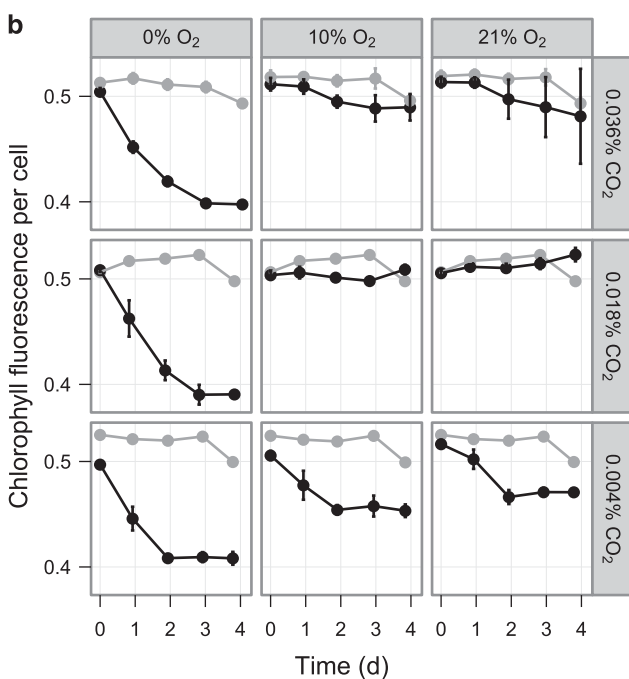


Figure 1 (a) *Prochlorococcus* MED4 cell concentration and (b) mean chlorophyll fluorescence per cell in cultures sparged with nine mixtures of O₂ and CO₂. All cultures were inoculated at *t* = 1 day. Experimental cultures (black) were sparged with the indicated gas mix (balanced with N₂), beginning at *t* = 0 days; control cultures (gray) were inoculated and grown in parallel but not sparged. Data points are the mean of at least three cultures. Error bars indicate 1 s.d.; where error bars are not visible, they are smaller than the plotting symbol. The drop in chlorophyll fluorescence per cell in control cultures from *t* = 3 days to *t* = 4 days is expected for cultures entering stationary phase. In experimental cultures, the addition of CO₂ is expected to delay this transition (Moore *et al.*, 2007).

experiment's extremes: media sparged with 0.004% CO₂+21% O₂ (hereafter, -CO₂ shock), 0.004% CO₂+<0.001% O₂ (-CO₂/−O₂ shock) and 0.036% CO₂+<0.001% O₂ (-O₂ shock). We used an empirical Bayes approach to detect changes in expression (Aryee *et al.*, 2009), explicitly including the time dependence of samples within each condition to identify genes whose expression profiles over the time course differed significantly (*P*-value threshold, 0.98; false discovery rate, 0.02) from baseline. Within the air control, the baseline was expression at *t* = 0; for the experimental conditions, the baseline was the full profile in air.

General patterns. Within the air-sparged control, we observed differential expression of 188 genes, including 67 hypothetical genes (Supplementary Table S1). These changes were typically small (Supplementary Table S1) and may reflect the stress of centrifugation immediately before the *t* = 0 time-point. Differential expression with respect to air was minimal under -O₂ shock (4 of 2048 genes probed) but widespread under -CO₂ shock (296 genes) and -CO₂/−O₂ shock (261 genes) (Figure 2a, Supplementary Table S1). Although the latter two sets of genes overlap substantially, sharing 184 genes, clustering analysis of relative expression patterns in shock conditions with respect to air revealed an oxygen dependence to the expression



profiles of many genes under carbon limitation (Figure 2b). Under -CO₂/−O₂ shock, sustained suppression of expression (cluster 4, 112 genes) was far more common than suppression with early recovery (cluster 3, 32 genes) among the differentially expressed genes; under -CO₂ shock, sustained suppression was slightly less common than early recovery (52 vs 66 genes), raising the possibility that oxygen availability partially mitigated the effects of carbon limitation on the timescale studied here.

As a first look at the relationship between the responses to upstream and downstream triggers of a photosynthetic imbalance, we examined the genes showing differential expression under acute high-light stress in earlier work (Steglich *et al.*, 2006, 2008) compared with those reported here for CO₂ limitation. There was very strong concordance in the direction of change: high light and -CO₂/−O₂ shock evoked congruent initial responses (increased high-light expression at *t* = 45 min and gas shock cluster 1, or decreased high-light expression and gas shock cluster 2, 3 or 4; Figure 2b) in 35 of 41 shared genes, and high light and -CO₂ shock did so in 44 of 46 (Supplementary Table S2). Among genes that responded to -CO₂/−O₂ shock, the distribution of genes across clusters 2–4 was no different for genes that did respond to light stress than for those that did not (*P* = 0.387, Fisher's exact test). By contrast, among all genes whose expression initially dropped

under -CO₂ shock, those that also responded to light stress were significantly more likely to recover rapidly even as CO₂ limitation continued (cluster 3; $P=0.012$, Fisher's exact test). That is, access to oxygen appears to reduce the extent to which CO₂ limitation mimics high-light stress. As described below, this conclusion is borne out by closer

examination of the groups of genes affected by -CO₂ and -CO₂/−O₂ shock.

Hli gene family. The *hli* gene family encodes small proteins thought to interact with the photosystems under oxidative stress conditions (He *et al.*, 2001; Yao *et al.*, 2007). Named for their high-light inducibility, *hli* genes in MED4 have been induced by phage infection, N starvation, Fe starvation and a range of light shocks (Steglich *et al.*, 2006; Tolonen *et al.*, 2006; Lindell *et al.*, 2007; Thompson *et al.*, 2011), suggesting a more general role in stress response. We found that expression of six *hli* genes decreased after $t=0$ in the air control (Figure 3), and interpret this drop as a recovery to baseline after upregulation due to sample-handling stresses (centrifugation and resuspension) just before the $t=0$ timepoint. By contrast, expression of these *hli* genes remained at or above $t=0$ levels throughout the -CO₂/−O₂ time course, suggesting that this condition did not permit recovery to a non-stressed state.

Under carbon limitation, the large majority of differentially expressed *hli* genes showed a persistent and strong increase in expression with respect to air (-CO₂, 11 of 12 differentially expressed *hli* genes in cluster 1; -CO₂/−O₂, 10 of 11), but *hli3* (PMM1482) was an intriguing exception. MED4's *hli* suite is dominated by multi-copy genes (Bhaya *et al.*, 2002; Lindell *et al.*, 2004), which respond to a variety of stimuli (Tolonen *et al.*, 2006; Steglich *et al.*, 2006; Lindell *et al.*, 2007; Thompson *et al.*, 2011). Their presence in genomic islands (Coleman *et al.*, 2006) and phage suggests that they are exchanged through horizontal gene transfer, forming part of the highly niche-dependent 'flexible' genome (Kettler *et al.*, 2007). By contrast, the five single-copy *hli* genes, including *hli3*, belong to the core genome and have never previously been seen to respond to a stress condition in MED4 (Steglich *et al.*, 2006; Tolonen *et al.*, 2006; Lindell *et al.*, 2007; Thompson *et al.*, 2011; Kettler, personal communication). Here, both carbon limitation conditions strongly

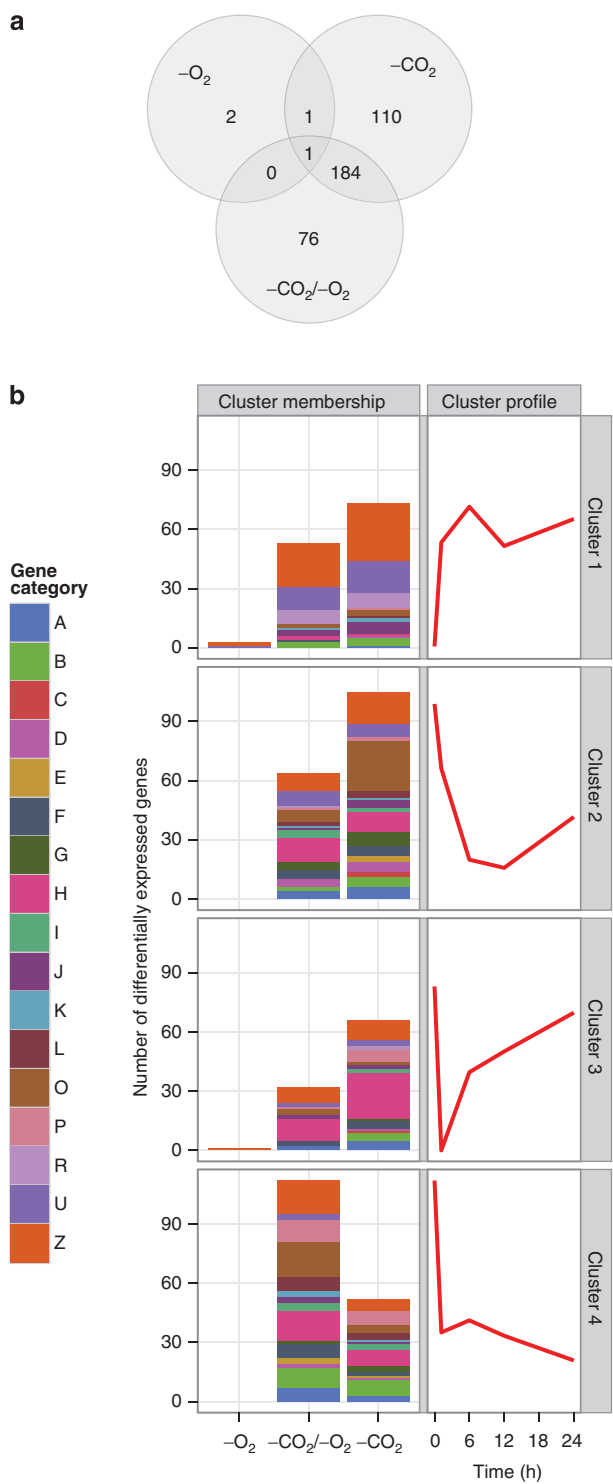


Figure 2 (a) Results of whole-genome transcriptional profiling in the gas shock experiment. Venn diagram of genes showing significant differential expression with respect to air in the three experimental conditions: -O₂ shock (0.036% CO₂, 0% O₂), -CO₂ shock (0.004% CO₂, 21% O₂) and -CO₂/−O₂ shock (0.004% CO₂, 0% O₂). (b) Clustering analysis of changes in gene expression under gas shocks relative to changes in air. Autoscaled cluster centroids are shown at right, in red. Clusters 2 and 3 are categorized as showing suppression and subsequent recovery. At left, bar plots give the number of genes in each cluster under each gas shock condition. Gene categories: A, amino-acid biosynthesis; B, biosynthesis of cofactors, prosthetic groups, and carriers; C, cell envelope; D, cellular processes; E, central intermediary metabolism; F, energy metabolism; G, fatty acid, phospholipid, and sterol metabolism; H, photosynthesis and respiration; I, purines, pyrimidines, nucleosides, and nucleotides; J, regulatory functions; K, DNA replication, recombination, and repair; L, transcription; O, translation; P, transport and binding proteins; R, RNA; U, other categories; Z, hypothetical proteins.

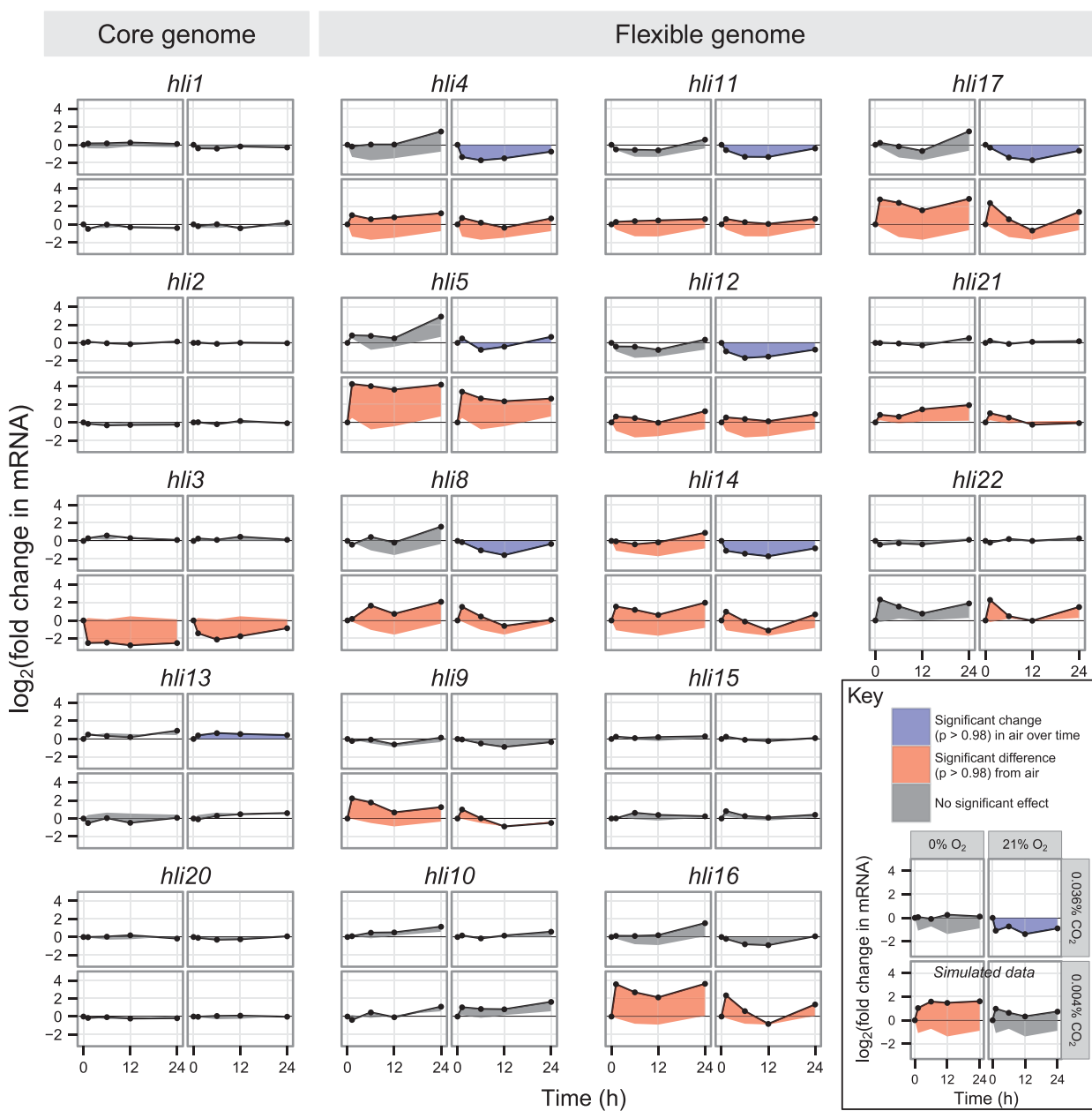


Figure 3 Expression of high-light-inducible (*hli*) genes of the core (left) and flexible (right) MED4 genome in the gas shock experiment. Data points are the geometric means of two biological replicates. Fold change is relative to $t = 0$ for each condition. All thumbnail plots share the same layout; for details, see sample plot at lower right. Data in sample plot (see Key) is simulated for illustration. The region between each time course and the baseline used for significance testing (for the air control, expression at $t = 0$; for experimental conditions, the parallel time course in air) is shaded according to the outcome of that test: a significant change in expression in air with respect to $t = 0$, blue; a significantly different time course in an experimental condition than in air, red; no significant effect, gray.

suppressed *hli3* expression (Figure 3). The direction of this change substantiates the idea that *hli* genes in the core and flexible genomes have fundamentally different roles (Zinser *et al.*, 2009).

Regulatory genes. Under both $-CO_2$ and $-CO_2/O_2$ shocks, RNA polymerase genes (*rpoABC1C2*) were significantly downregulated, likely contributing to a broad suppression of transcription (Figure 1, Supplementary Figure S1). The translational machinery was likewise substantially suppressed under both

conditions, with roughly half the 30S and a third of 50S ribosome genes showing lowered expression (Supplementary Figure S2, Supplementary Table S1). Consistent with these changes, *groEL* and *groEL2*, components of the GroEL chaperone for newly synthesized proteins, were also expressed at lower levels (Supplementary Table S1). Despite these broad similarities, we observed some distinct regulatory responses to the stresses. The type II alternative sigma factor encoded by PMM1289 has previously been found to show differential responses

to nutrient stresses, with transcript abundance increasing in the early hours of N starvation but not in response to P starvation (Martiny *et al.*, 2006; Tolonen *et al.*, 2006). Here, PMM1289 was significantly upregulated in -CO₂ stress only (Supplementary Figure S1), suggesting that CO₂ limitation in the presence of oxygen triggers invocation of a different transcriptional program than does co-limitation of CO₂ and O₂.

Mean expression of the Crp-family gene at locus PMM0806 showed a >4-fold increase in expression under -CO₂ shock, while dropping by nearly 4-fold under both -O₂ shock and -CO₂/ -O₂ shock

(Figure 4a). Although these decreases failed to meet our conservative differential expression threshold with respect to air, the difference between expression under -CO₂ shock and under the oxygen limitation conditions was highly significant ($P=1$, false discovery rate controlled at 0.001). Crp-family proteins are transcriptional regulators, typically activators, controlled by a range of signals including cAMP, redox potential, and O₂ (Körner *et al.*, 2003). The highly oxygen-dependent transcriptional response we observe, together with previous experiments demonstrating PMM0806 induction under iron limitation (Thompson *et al.*, 2011), strongly

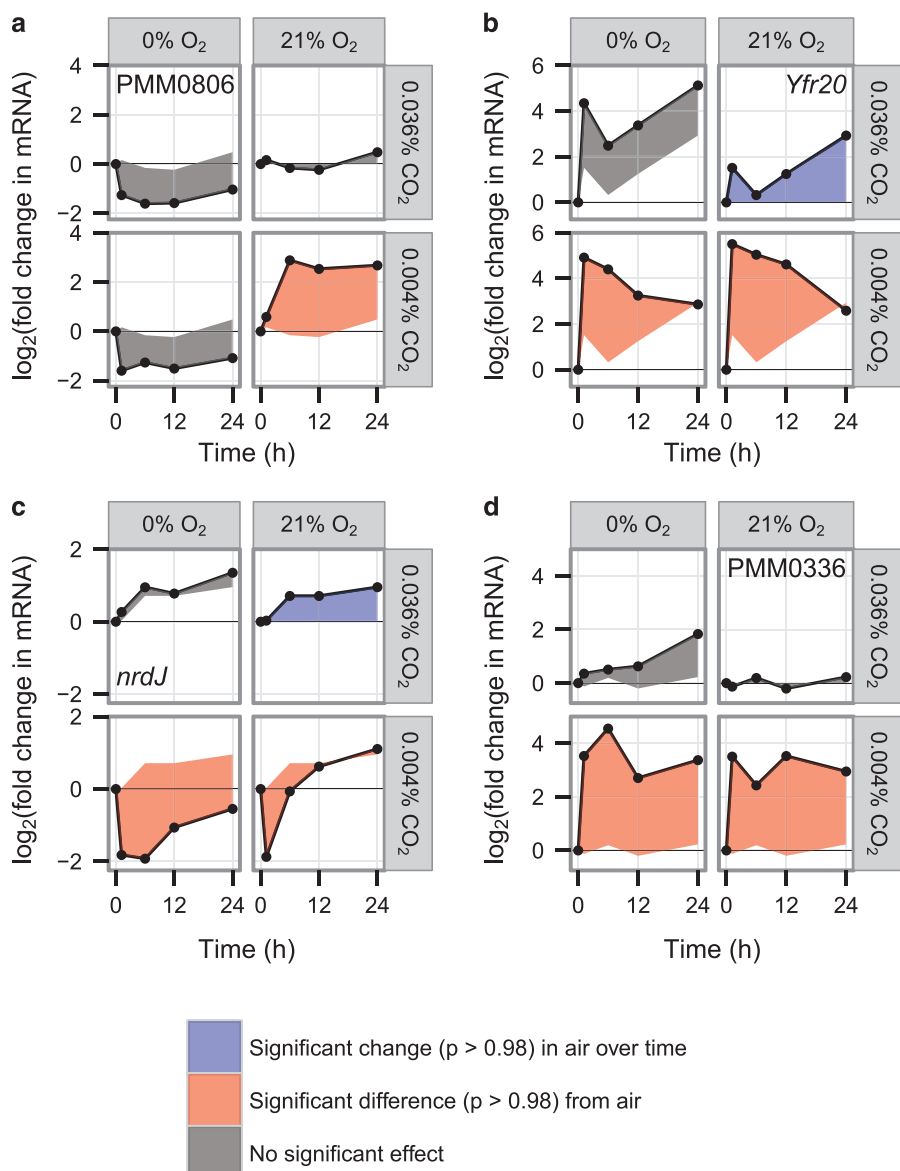


Figure 4 Expression of (a) the putative CRP-family regulatory gene encoded by MED4 locus PMM0806, (b) Yfr20, (c) *nrdJ*, and (d) the PTOX locus PMM0336 in the gas shock experiment. Data points are the geometric means of two biological replicates. Fold change is relative to $t=0$ for each condition. The region between each time course and the baseline used for significance testing (for the air control, expression at $t=0$; for experimental conditions, the parallel time course in air) is shaded according to the outcome of that test: a significant change in expression in air with respect to $t=0$, blue; a significantly different time course in an experimental condition than in air, red; no significant effect, gray.

suggests that PMM0806 expression responds to a redox-related signal.

Although genome streamlining has left *Prochlorococcus* with a minimal complement of regulatory proteins, its complement of non-coding and anti-sense RNA genes is comparable to those of well-studied enterobacteria (Steglich *et al.*, 2008) and is expected to have a major role in regulation. Here, a few antisense RNA genes were differentially expressed, but these patterns showed little clear relation to the expression of their target genes (Supplementary Figure S3). Strikingly, however, the strongest response observed for any gene was the ~30-fold upregulation of the non-coding RNA Yfr20 under both -CO₂ and -CO₂/−O₂ shock (Figure 4b). Yfr20 is common to high-light *Prochlorococcus* strains and has previously been observed to be very strongly induced by high-light stress (Steglich *et al.*, 2008).

Carbon transport and fixation. *Prochlorococcus* has few known transporters for inorganic carbon (Ci) (Scanlan *et al.*, 2009). Like most open-ocean cyanobacteria, MED4 lacks inducible high-affinity Ci uptake systems, likely reflecting the relative homogeneity of Ci levels in pelagic waters as compared with coastal and lacustrine systems (Badger *et al.*, 2006; Scanlan *et al.*, 2009). Instead, MED4's Ci acquisition is expected to depend primarily on the Na⁺/HCO₃⁻ symporter BicA (PMM0214) (Badger *et al.*, 2002, 2006; Price *et al.*, 2004; Hopkinson *et al.*, 2014). Although minimal, this Ci uptake machinery contributes to a highly efficient carbon-concentrating mechanism; its half-saturation point for uptake has recently been measured at 80–130 μM HCO₃⁻ (Hopkinson *et al.*, 2014). With pH controlled at 8.1, both CO₂ limitation conditions should give [HCO₃⁻] ~ 213 μM, theoretically within the saturation regime. That we observe marked growth limitation and a substantial transcriptional stress response at this CO₂ level suggests either that the half-saturation point is higher under our culture conditions or that, even at moderate cell densities (~5 × 10⁷ cells ml⁻¹), photosynthesis renders bubbling insufficient to maintain pCO₂ at 40 μatm (Shi and Xu, 2009) and HCO₃⁻ at saturating concentrations. Whatever the mechanism of the limitation, its effect on MED4's carbon-concentrating mechanism is remarkable: expression of *bicA* dropped rapidly and remained suppressed under both -CO₂ and -CO₂/−O₂ shock (Supplementary Table S1). No other candidate cryptic Ci transporters (Harano *et al.*, 1997; Palinska *et al.*, 2002; Shibata *et al.*, 2002; Scanlan *et al.*, 2009) were induced by CO₂ limitation. It is difficult to rationalize this strategy if we assume that MED4 is directly sensing Ci availability, but given MED4's extensive genome streamlining that assumption is likely false: the environmental Ci concentrations *Prochlorococcus* encounters should consistently be well above saturating for Ci uptake,

such that direct Ci sensing is unlikely to offer a selective advantage.

Both carbon limitation conditions also caused broad transcriptional suppression of the machinery necessary for carbon fixation. Fixation places a heavy demand for ATP production on the cell, high enough that ATP synthase expression during daytime carbon fixation exceeds expression during nighttime aerobic respiration (Zinser *et al.*, 2009). Under both carbon limitation conditions, expression of 9 of the 10 ATP synthase complex genes (at loci PMM1438–1439 and PMM1450–1457) was significantly decreased (Supplementary Table S1), with similar time course profiles across the two conditions. We further observed decreased expression of genes encoding Calvin cycle enzymes (Figure 5), several carboxysome components (*csoS1* (PMM0549), *csoS2* (PMM0552), *csoSCA* (PMM0553), and *csoS4B* (PMM0553); Supplementary Table S1), and glycogen synthesis enzymes (*glgABC*, encoded by PMM0609, PMM0584 and PMM0769, respectively; Supplementary Table S1) under CO₂ limitation. However, the availability of oxygen appears to modulate this response: while Calvin cycle gene expression was reduced under both carbon limitation conditions, the effect was generally stronger and more sustained under -CO₂/−O₂ shock than under -CO₂ shock (Figure 5). This disparity is most striking in the Rubisco genes *rbcLS*. As discussed below, the minimal disruption of Rubisco expression under -CO₂ shock suggests that, with carbon fixation throttled, the availability of molecular oxygen allows *Prochlorococcus* to buffer light stress via Rubisco's oxygenation reaction.

Photosystems. Halting carbon fixation slows NADPH consumption, threatening the photosynthetic electron transport chain with over-reduction. Two-thirds of the genes encoding proteins in the light-harvesting complex and PSI and PSII were differentially expressed under carbon limitation (-CO₂/−O₂ shock, 15 of 34 genes; -CO₂ shock, 19; total, 22). Of these, all were initially suppressed relative to air (Supplementary Table S1); but whereas just over half the photosystem genes suppressed under -CO₂/−O₂ shock remained suppressed (cluster 4; Figures 2b and 6), nearly all photosystem genes affected by -CO₂ shock recovered sharply and substantially (cluster 3; Figures 2b and 6). The same pattern marked cytochrome b_{6f} and nicotinamide nucleotide transhydrogenase (*pntA1*, *pntA2* and *pntB*), which couples the proton gradient to the transfer of reducing equivalents between the NAD(H) and NADP(H) pools (Figure 6b). The expression profiles seen throughout the photosynthetic electron transport chain—sustained suppression under -CO₂/−O₂, suppression with recovery under -CO₂—strongly suggest that, in carbon-limited cells, access to oxygen affects the health of this system.

Cyanobacterial iron physiology is closely tied to photosystem status (Thompson *et al.*, 2011), and

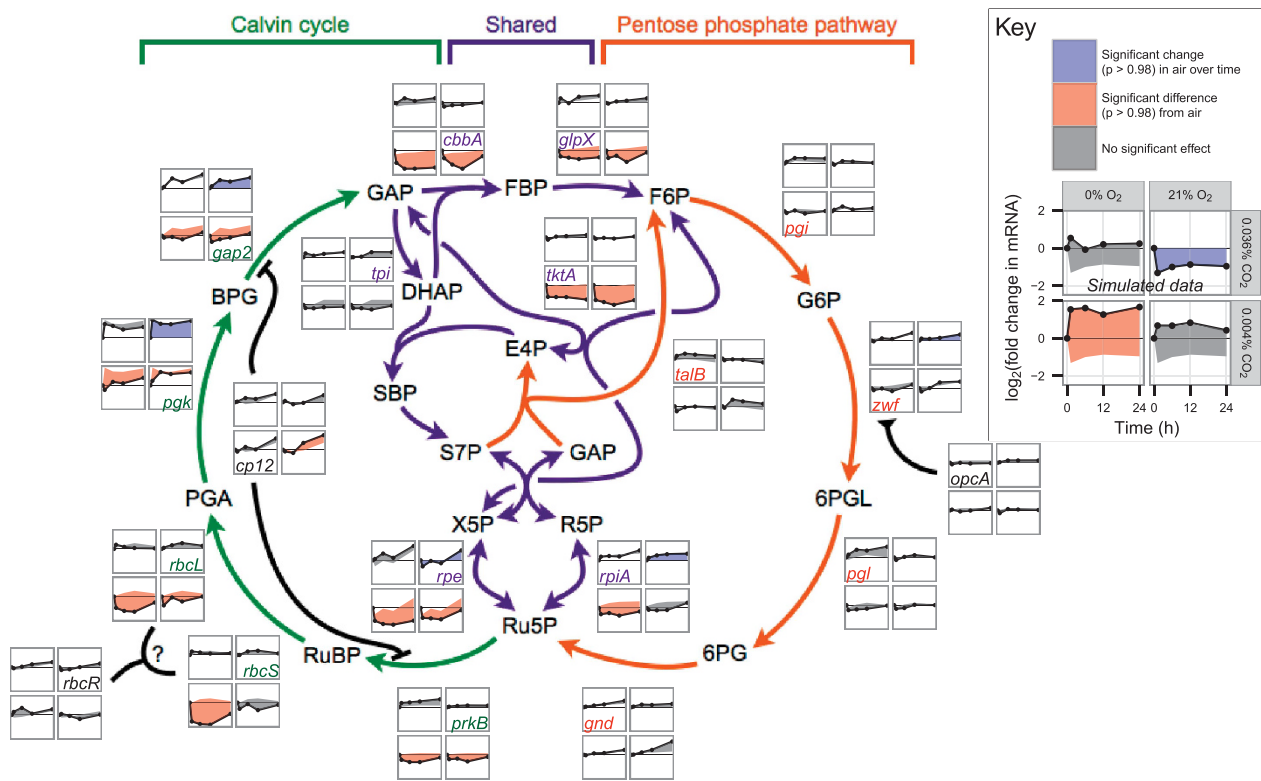


Figure 5 Expression of Calvin cycle and pentose phosphate pathway genes. The Calvin cycle (green) and pentose phosphate pathway (orange) interlock; because their shared reactions (purple) run in opposite directions, the cycles cannot productively run at the same time. Gas shock expression data (thumbnail plots) for each gene in these pathways suggests that, as expected, CO₂ starvation broadly downregulates the carbon-fixing Calvin cycle, while leaving the reductive pentose phosphate pathway largely intact. Data points are the geometric means of two biological replicates. Fold change is relative to $t=0$ for each condition. All thumbnail plots share the same layout and axis scales; for details, see sample plot at lower right. Data in sample plot (see Key) is simulated for illustration. The region between each time course and the baseline used for significance testing (for the air control, expression at $t=0$; for experimental conditions, the parallel time course in air) is shaded according to the outcome of that test: a significant change in expression in air with respect to $t=0$, blue; a significantly different time course in an experimental condition than in air, red; no significant effect, gray. Genes: *cbbA*, fructose-1,6-bis-P:sedoheptulose-1,7-bis-P aldolase; *cp12*, regulator CP12; *gap2*, glyceraldehyde-3-phosphate dehydrogenase; *glpX*, fructose-1,6/sedoheptulose-1,7-bisphosphatase; *gnd*, 6-phosphogluconate dehydrogenase; *opcA*, putative glucose-6-phosphate dehydrogenase effector; *pgi*, P-glucose isomerase; *pgk*, P-glycerate kinase; *pgl*, 6-P-gluconolactonase; *prkB*, P-ribulokinase; *rbcLS*, ribulose-1,5-bis-P carboxylase/oxygenase large and small subunits; *rbcR*, putative Rubisco transcriptional regulator; *rpe*, ribulose-5-P epimerase; *rpiA*, ribulose-5-P isomerase; *talB*, transaldolase; *tktA*, transketolase; *tpi*, triose-P isomerase; *zwf*, glucose-6-phosphate dehydrogenase. Substrates: BPG, 2,3-bis-P-glycerate; DHAP, dihydroxyacetone P; E4P, erythrose-4-P; FBP, fructose-1,6-bis-P; F6P, fructose-6-P; GAP, glyceraldehyde-3-P; G6P, glucose-6-P; PGA, 3-P-glyceric acid; R5P, ribose-5-P; RuBP, ribulose-1,5-bis-P; Ru5P, ribulose-5-P; SBP, sedoheptulose-1,7-bis-P; 6PG, 6-P-gluconate; 6PGL, 6-P-gluconolactone; S7P, sedoheptulose-7-P; and X5P, xylulose-5-P.

again, we observe divergent responses under -CO₂ and -CO₂/−O₂ shocks. Expression of the gene encoding the iron sequestration protein ferritin (PMM0804) and of one ferric uptake regulator (Fur) gene (PMM1030) increased significantly only under -CO₂, whereas the other Fur gene (PMM0637) was upregulated more strongly under -CO₂ shock than -CO₂/−O₂ shock (Supplementary Table S1). Unusually for regulatory proteins, Fur is typically expressed at high copy number; each subunit binds one Fe(III) ion, so upregulation contributes directly to iron sequestration (Andrews *et al.*, 2003). Oxygen-dependent differences in the expression of these genes under carbon limitation are consistent with distinct patterns of photosystem remodeling under -CO₂ and -CO₂/−O₂ shocks.

DNA synthesis. One gene related to DNA synthesis also showed oxygen-dependent recovery under carbon limitation: the class II ribonucleotide reductase *nrdJ* (PMM0661) (Figure 4c). Ribonucleotide reductases convert ribonucleotides to deoxyribonucleotides, preparing the cell for DNA replication and cell division. The strong initial decrease in *nrdJ* transcript abundance under both -CO₂ and -CO₂/−O₂ shocks was consistent with the expectation that severe carbon limitation would halt cell division. But why should *nrdJ* expression then fully recover under -CO₂ shock? Intriguingly, in the obligate aerobe *Streptomyces coelicolor*, *nrdJ* activity is essential for rapid recovery after oxygen starvation (Borovok *et al.*, 2004); ongoing deoxyribonucleotide synthesis may prepare the cell to begin DNA

synthesis as soon as environmental conditions permit. If the same is true in *Prochlorococcus*, cultures released from -CO₂ shock would be primed for recovery, whereas those released from -CO₂/-O₂ shock would not.

Opening safety valves under carbon limitation: PTOX and 2-phosphoglycolate

When energy cannot flow from photons to reducing equivalents to carbon–carbon bonds, the cell risks

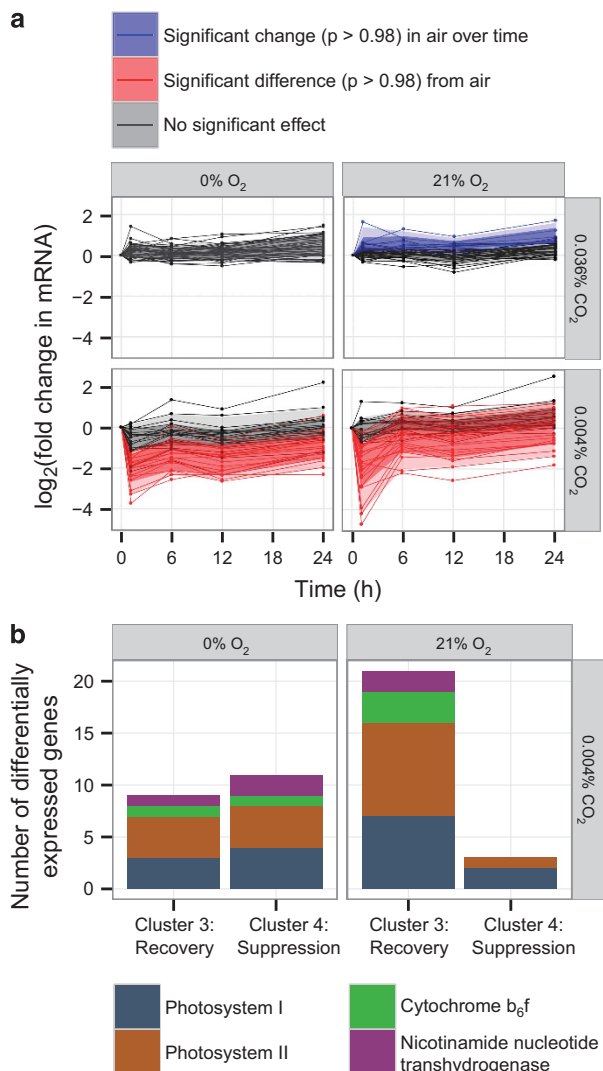


Figure 6 (a) Expression of MED4 genes encoding PSI and PSII, cytochrome b₆f and pnt genes in the gas shock experiment. Data points are the geometric means of two biological replicates. Fold change is relative to t=0 for each condition. Shock conditions causing significant differential expression in the air control with respect to time 0 are highlighted in blue; shock conditions causing significant differential expression over the time course with respect to air are highlighted in red. Ninety percent of data points lie within the outer (light) shaded bands; 70% lie within the inner (dark) bands. (b) Oxygen dependence of the cluster affiliations of the genes in panel a under carbon limitation. No differentially expressed genes in this set fell into cluster 1 (increased expression) or 2 (delayed recovery). See Figure 2b for cluster profiles.

widespread damage. Of the protective strategies thought to be available to *Prochlorococcus* (Scanlan *et al.*, 2009), no mechanism is yet known for non-photochemical quenching, and we find no indication at the transcriptional level that carbon limitation modulates cyclic electron flow or the Mehler reaction, with 13 of 14 ndh genes, flv1 (PMM0042), and flv3 (PMM0043) unchanged under -CO₂ and -CO₂/-O₂ shocks. Instead, carbon-limited MED4 appears to use two photo-protective strategies, both relying on oxygen (Figure 7). These strategies may explain why light-stress-related genes whose expression initially responded to CO₂ limitation were disproportionately likely to recover in cultures with access to exogenous O₂.

First, PSII can pass electrons to oxygen instead of cytochrome b₆f via the plastoquinol terminal oxidase (PTOX, PMM0336), a strategy demonstrated in *Synechococcus* WH8102 cultures and observed in an iron-limited open-ocean cyanobacterial population dominated by *Prochlorococcus* (Bailey *et al.*, 2008; Mackey *et al.*, 2008). Previous *Prochlorococcus* transcriptome experiments have shown PTOX upregulation when iron limitation induced PSI down-regulation (Thompson *et al.*, 2011) and when light shocks threatened PSII and the plastoquinone (PQ) pool with over-reduction (Steglich *et al.*, 2006). By contrast, when the PSII inhibitor DCMU was used to trap PQ in an oxidized state, PTOX transcription was significantly repressed (Steglich *et al.*, 2006). Here, PTOX expression increased >11-fold under both -CO₂ and -CO₂/-O₂ shocks (Figure 4d). Interpretation of this result is difficult for -CO₂/-O₂ shock: PSII may have continued to generate molecular oxygen, but given the steep gradient for diffusive loss to the 0% O₂ medium, little of that oxygen may have been

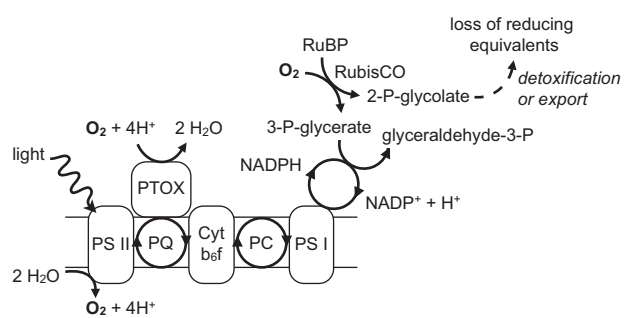


Figure 7 Proposed ‘safety valves’ for carbon-limited *Prochlorococcus*. Light energy drives the photosynthetic electron transport chain, transferring reducing power from PSII via PQ to cytochrome b₆f (Cyt b₆f); from there via plastocyanin (PC) to PSI; and from there to the NADPH pool. In the presence of CO₂, carbon fixation provides a final sink for these reducing equivalents; in its absence, the electron transport chain can divert excess electrons from PQ to O₂ via the PQ terminal oxidase (PTOX), or ribulose-1,5-bisphosphate (RuBP) can be oxygenated, forcing the consumption of reducing equivalents to process the products.

available to PTOX. With transcriptional data alone, we cannot say whether continued PTOX expression under -CO₂/–O₂ shock represented maintenance of a successful strategy or the futile result of signaling from an electron transport chain under continuing stress. But the broader patterns of O₂-dependent transcriptional recovery suggest that any PTOX activity achieved under -CO₂/–O₂ shock was insufficient. If, like *Synechococcus elongatus*, *Prochlorococcus* uses PQ redox poise as a signaling input (Kim *et al.*, 2012), different rates of PTOX activity in the presence and absence of exogenous O₂ may have had a major role in triggering the different transcriptional programs observed under -CO₂ and -CO₂/–O₂ shocks.

Second, *Prochlorococcus* can exploit Rubisco's oxygenation reaction to produce one 3-phosphoglycerate and one 2-phosphoglycolate. The former can be recycled through the Calvin cycle, consuming NADPH directly; the latter must be either detoxified via photorespiration or expelled. Although photorespiration appears to be essential in some cyanobacteria (Eisenhut *et al.*, 2008), MED4, like most sequenced *Prochlorococcus* strains, lacks some components of the known detoxification pathways (Scanlan *et al.*, 2009); moreover, it is known to secrete substantial quantities of glycolate even under exponential growth (Bertilsson *et al.*, 2005). Whereas PTOX may retain some activity under -CO₂/–O₂ shock through use of the photosynthetic O₂ generated nearby, the sequestration of Rubisco within carboxysomes makes any use of this safety valve highly unlikely when cellular O₂ is low. Consistent with this, *rbcLS* were strongly (~4-fold) downregulated under -CO₂/–O₂ shock; but under -CO₂ shock, *rbcS* was not significantly affected, and *rbcL* expression dropped but rapidly recovered (cluster 3, Figures 2b and 5).

We find no evidence for increased expression of reactive oxygen species scavengers under carbon limitation (data not shown), leaving cells without photoprotection vulnerable to mounting oxidative damage. In some heterotrophs, reactive oxygen species defense during starvation is necessary for recovery thereafter (McDougald *et al.*, 2002). The effect may be the same in *Prochlorococcus*: the expression pattern of *nrdJ*, discussed above, suggests that only MED4 cells with O₂ access could prepare for recovery from CO₂ starvation. But why should MED4 need the ability to recover from CO₂ starvation at all, when it is unlikely ever to encounter such low CO₂ levels in the oligotrophic ocean? The concordance between the CO₂ limitation and light stress responses, including their shared extremely strong expression of the non-coding RNA Yfr20, points to the conclusion that, on short (<1 day) timescales, the relevant factor is not the absolute CO₂ concentration but the balance between CO₂ and irradiance.

Threats to this central balance would be part of daily life for *Prochlorococcus* populations in tropical

surface waters, so the ability to recover after a few hours' exposure to a photosynthetic impedance mismatch may be highly adaptive. If this is true, access to oxygen and the safety valve machinery should be most important in surface waters; conversely, exogenous oxygen may be dispensable at the very low irradiances that penetrate to oxygen minimum zones. Notably, although PTOX homologs are widespread in high-light-adapted *Prochlorococcus*, the only low-light-adapted *Prochlorococcus* ecotype known to carry a PTOX homolog is the LLI clade, whose members are abundant in some deeply mixed surface waters (Zinser *et al.*, 2007; Scanlan *et al.*, 2009).

Though a photosynthetic impedance mismatch may be a regular environmental stress for *Prochlorococcus*, a mismatch lasting continuously for >1 day is an impossibility, and the ability to withstand such a stress will not have been under selection. Here, the timing of the shifts observed in the growth experiment (Figure 1) bears further examination. From *t*=0 to 1 day, MED4 cells at 0.004% CO₂ and 21% O₂ tracked closely with the controls in both growth and per-cell chlorophyll fluorescence. Beyond 1 day in constant light, cell density increased no further, and per-cell chlorophyll fluorescence fell off. Although constant, the irradiance used in this study was too low (~60 μmol photons m⁻² s⁻¹) to provoke photoinhibition in carbon-replete and oxygen-replete MED4 (Moore and Chisholm, 1999); but lack of exogenous O₂ provokes a substantial drop in per-cell chlorophyll fluorescence at all CO₂ levels within 1 day of constant light, and a slowing of growth within 2 days. Oxygen-dependent safety valves may thus be essential not only for recovery from severe but transient imbalances between irradiance and carbon fixation capacity but also for the maintenance of normal photosynthetic electron transport in carbon-replete cells in moderate light.

Although the carbon limitation used in these experiments is far more extreme than *Prochlorococcus* would ever experience in nature, our results suggest that the resulting general stress is a familiar one, perhaps even daily for marine populations in low latitudes. Whether the photosynthetic electron transfer chain is threatened by increasing irradiance or throttling carbon fixation, the cell must dissipate an excess of reducing equivalents to survive. For *Prochlorococcus* MED4, the cell's capacity to respond and recover appears to hinge on oxygen. To explore this response, future work should directly measure NAD(P)/NAD(P)H balance, pigment content, and the maximum photosynthetic quantum yield (Fv/Fm) in the presence and absence of exogenous O₂ across a range of CO₂ levels and irradiances. The recovery phase will be of particular interest: for severely CO₂-limited cells, could recovery be initiated simply by turning out the lights?

Conflict of Interest

The authors declare no conflict of interest.

Acknowledgements

This work was supported by grants from the US Department of Energy—GTL, NSF Biological Oceanography, NSF Center for Microbial Oceanography Research and Education (C-MORE), the Seaver Foundation and the Gordon and Betty Moore Foundation. SCB was an HHMI Pre-doctoral Fellow. We thank Jessica Wiedemier Thompson, Rogier Braakman, Qinglu Zeng, Luke Thompson, and Brian Hopkinson for their helpful comments on the manuscript.

References

- Andrews SC, Robinson AK, Rodríguez-Quiñones F. (2003). Bacterial iron homeostasis. *FEMS Microbiol Rev* **27**: 215–237.
- Aryee MJ, Gutiérrez-Pabello JA, Kramnik I, Maiti T, Quackenbush J. (2009). An improved empirical bayes approach to estimating differential gene expression in microarray time-course data: BETR (Bayesian Estimation of Temporal Regulation). *BMC Bioinformatics* **10**: 409.
- Axmann IM, Dühring U, Seeliger L, Arnold A, Vanselow JT, Kramer A et al. (2009). Biochemical evidence for a timing mechanism in *Prochlorococcus*. *J Bacteriol* **191**: 5342–5347.
- Badger MR, Hanson D, Price GD. (2002). Evolution and diversity of CO₂ concentrating mechanisms in cyanobacteria. *Funct Plant Biol* **29**: 161–173.
- Badger MR, Price GD, Long BM, Woodger FJ. (2006). The environmental plasticity and ecological genomics of the cyanobacterial CO₂ concentrating mechanism. *J Exp Bot* **57**: 249–265.
- Bailey S, Melis A, Mackey KRM, Cardol P, Finazzi G, van Dijken G et al. (2008). Alternative photosynthetic electron flow to oxygen in marine *Synechococcus*. *Biochim Biophys Acta* **1777**: 269–276.
- Bertilsson S, Berglund O, Pullin MJ, Chisholm SW. (2005). Release of dissolved organic matter by *Prochlorococcus*. *Vie Milieu Paris* **55**: 225–231.
- Bhaya D, Dufresne A, Vaulot D, Grossman A. (2002). Analysis of the *hlj* gene family in marine and freshwater cyanobacteria. *FEMS Microbiol Lett* **215**: 209–219.
- Bolstad BM, Irizarry RA, Åstrand M, Speed TP. (2003). A comparison of normalization methods for high density oligonucleotide array data based on variance and bias. *Bioinformatics* **19**: 185–193.
- Borovok I, Gorovitz B, Yanku M, Schreiber R, Gust B, Chater K et al. (2004). Alternative oxygen-dependent and oxygen-independent ribonucleotide reductases in *Streptomyces*: cross-regulation and physiological role in response to oxygen limitation. *Mol Microbiol* **54**: 1022–1035.
- Bowes G, Ogren WL, Hageman RH. (1971). Phosphoglycolate production catalyzed by ribulose diphosphate carboxylase. *Biochem Biophys Res Commun* **45**: 716–722.
- Coleman ML, Sullivan MB, Martiny AC, Steglich C, Barry K, DeLong EF et al. (2006). Genomic islands and the ecology and evolution of *Prochlorococcus*. *Science* **311**: 1768–1770.
- Coleman ML, Chisholm SW. (2007). Code and context: *Prochlorococcus* as a model for cross-scale biology. *Trends Microbiol* **15**: 398–407.
- Dinsdale EA, Pantos O, Smriga S, Edwards RA, Angly F, Wegley L et al. (2008). Microbial ecology of four coral atolls in the Northern Line Islands. *PLoS One* **3**: e1584.
- Dufresne A, Salanoubat M, Partensky F, Artiguenave F, Axmann IM, Barbe V et al. (2003). Genome sequence of the cyanobacterium *Prochlorococcus marinus* SS120, a nearly minimal oxyphototrophic genome. *Proc Natl Acad Sci USA* **100**: 10020–10025.
- DuRand MD, Green RE, Sosik HM, Olson RJ. (2002). Diel variations in optical properties of *Micromonas pusilla* (Prasinophyceae). *J Phycol* **38**: 1132–1142.
- Eisenhut M, Ruth W, Haimovich M, Bauwe H, Kaplan A, Hagemann M. (2008). The photorespiratory glycolate metabolism is essential for cyanobacteria and might have been conveyed endosymbiotically to plants. *Proc Natl Acad Sci USA* **105**: 17199–17204.
- Futschik ME, Carlisle B. (2005). Noise-robust soft clustering of gene expression time-course data. *J Bioinform Comput Biol* **3**: 965–988.
- Goericke R, Olson RJ, Shalapyonok A. (2000). A novel niche for *Prochlorococcus* sp. in low-light suboxic environments in the Arabian Sea and the Eastern Tropical North Pacific. *Deep Sea Res Part 1 Oceanogr Res Pap* **47**: 1183–1205.
- Harano Y, Suzuki I, Maeda S, Kaneko T, Tabata S, Omata T. (1997). Identification and nitrogen regulation of the cyanase gene from the cyanobacteria *Synechocystis* sp. strain PCC 6803 and *Synechococcus* sp. strain PCC 7942. *J Bacteriol* **179**: 5744–5750.
- He Q, Dolganov N, Björkman O, Grossman AR. (2001). The high light-inducible polypeptides in *Synechocystis* PCC6803: Expression and function in high light. *J Biol Chem* **276**: 306–314.
- Holtzendorff J, Partensky F, Mella D, Lennon J-F, Hess WR, Garczarek L. (2008). Genome streamlining results in loss of robustness of the circadian clock in the marine cyanobacterium *Prochlorococcus marinus* PCC 9511. *J Biol Rhythms* **23**: 187–199.
- Hopkinson BM, Young JN, Tansik AL, Binder BJ. (2014). The minimal CO₂ concentrating mechanism of *Prochlorococcus* MED4 is effective and efficient. *Plant Physiol* **166**: 2205–2217.
- Johnson Zi, Zinser ER, Coe A, McNulty NP, Woodward EMS, Chisholm SW. (2006). Niche partitioning among *Prochlorococcus* ecotypes along ocean-scale environmental gradients. *Science* **311**: 1737–1740.
- Kettler GC, Martiny AC, Huang K, Zucker J, Coleman ML, Rodrigue S et al. (2007). Patterns and implications of gene gain and loss in the evolution of *Prochlorococcus*. *PLoS Genet* **3**: e231.
- Kim Y-I, Vinyard DJ, Ananyev GM, Dismukes GC, Golden SS. (2012). Oxidized quinones signal onset of darkness directly to the cyanobacterial circadian oscillator. *Proc Natl Acad Sci USA* **109**: 17765–17769.
- Körner H, Sofia HJ, Zumft WG. (2003). Phylogeny of the bacterial superfamily of Crp-Fnr transcription regulators: exploiting the metabolic spectrum by controlling alternative gene programs. *FEMS Microbiol Rev* **27**: 559–592.
- Lavin P, González B, Santibáñez JF, Scanlan DJ, Ulloa O. (2010). Novel lineages of *Prochlorococcus* thrive within

- the oxygen minimum zone of the eastern tropical South Pacific. *Environ Microbiol Rep* **2**: 728–738.
- Li H, Sherman LA. (2000). A redox-responsive regulator of photosynthesis gene expression in the cyanobacterium *Synechocystis* sp. strain PCC 6803. *J Bacteriol* **182**: 4268–4277.
- Lindell D, Sullivan MB, Johnson ZI, Tolonen AC, Rohwer F, Chisholm SW. (2004). Transfer of photosynthesis genes to and from *Prochlorococcus* viruses. *Proc Natl Acad Sci USA* **101**: 11013–11018.
- Lindell D, Jaffe JD, Coleman ML, Futschik ME, Axmann IM, Rector T et al. (2007). Genome-wide expression dynamics of a marine virus and host reveal features of co-evolution. *Nature* **449**: 83–86.
- Mackey KRM, Paytan A, Grossman AR, Bailey S. (2008). A photosynthetic strategy for coping in a high-light, low-nutrient environment. *Limnol Oceanogr* **53**: 900–913.
- Malmstrom RR, Rodrigue S, Huang KH, Kelly L, Kern SE, Thompson A et al. (2013). Ecology of uncultured *Prochlorococcus* clades revealed through single-cell genomics and biogeographic analysis. *ISME J* **7**: 184–198.
- Martiny AC, Coleman ML, Chisholm SW. (2006). Phosphate acquisition genes in *Prochlorococcus* ecotypes: Evidence for genome-wide adaptation. *Proc Natl Acad Sci USA* **103**: 12552–12557.
- McDougald D, Gong L, Srinivasan S, Hild E, Thompson L, Takayama K et al. (2002). Defences against oxidative stress during starvation in bacteria. *Antonie Van Leeuwenhoek* **81**: 3–13.
- Mella-Flores D, Six C, Ratin M, Partensky F, Boutte C, Le Corguillé G et al. (2012). *Prochlorococcus* and *Synechococcus* have evolved different adaptive mechanisms to cope with light and UV stress. *Front Microbiol* **3**: 285.
- Moore LR, Goericke R, Chisholm SW. (1995). Comparative physiology of *Synechococcus* and *Prochlorococcus*: Influence of light and temperature on growth, pigments, fluorescence and absorptive properties. *Mar Ecol Prog Ser* **116**: 259–275.
- Moore LR, Chisholm SW. (1999). Photophysiology of the marine cyanobacterium *Prochlorococcus*: Ecotypic differences among cultured isolates. *Limnol Oceanogr* **44**: 628–638.
- Moore LR, Post AF, Rocap G, Chisholm SW. (2002). Utilization of different nitrogen sources by the marine cyanobacteria *Prochlorococcus* and *Synechococcus*. *Limnol Oceanogr* **47**: 989–996.
- Moore LR, Coe A, Zinser ER, Saito MA, Sullivan MB, Lindell D et al. (2007). Culturing the marine cyanobacterium *Prochlorococcus*. *Limnol Oceanogr Methods* **5**: 353–362.
- Morris JJ, Johnson ZI, Szul MJ, Keller M, Zinser ER. (2011). Dependence of the cyanobacterium *Prochlorococcus* on hydrogen peroxide scavenging microbes for growth at the ocean's surface. *PLoS One* **6**: e16805.
- Morris JJ, Lenski RE, Zinser ER. (2012). The Black Queen Hypothesis: evolution of dependencies through adaptive gene loss. *MBio* **3**: e00036–12.
- Naumann U, Luta G, Wand MP. (2010). The curvHDR method for gating flow cytometry samples. *BMC Bioinform* **11**: 44.
- Niyogi KK. (1999). Photoprotection revisited: Genetic and molecular approaches. *Annu Rev Plant Physiol Plant Mol Biol* **50**: 333–359.
- Palinska KA, Laloui W, Bédu S, Loiseaux-de Goërs S, Castets AM, Rippka R et al. (2002). The signal transducer P_{II} and bicarbonate acquisition in *Prochlorococcus marinus* PCC 9511, a marine cyanobacterium naturally deficient in nitrate and nitrite assimilation. *Microbiology* **148**: 2405–2412.
- Partensky F, Hess WR, Vaultot D. (1999). *Prochlorococcus*, a marine photosynthetic prokaryote of global significance. *Microbiol Mol Biol Rev* **63**: 106–127.
- Price GD, Woodger FJ, Badger MR, Howitt SM, Tucker L. (2004). Identification of a SulP-type bicarbonate transporter in marine cyanobacteria. *Proc Natl Acad Sci USA* **101**: 18228–18233.
- Price GD, Badger MR, Woodger FJ, Long BM. (2008). Advances in understanding the cyanobacterial CO₂-concentrating-mechanism (CCM): Functional components, Ci transporters, diversity, genetic regulation and prospects for engineering into plants. *J Exp Bot* **59**: 1441–1461.
- R Development Core Team (2010). R: A language and environment for statistical computing. <http://www.R-project.org/>.
- Roberts EW, Cai F, Kerfeld CA, Cannon GC, Heinhorst S. (2012). Isolation and characterization of the *Prochlorococcus* carboxysome reveal the presence of the novel shell protein CsoS1D. *J Bacteriol* **194**: 787–795.
- Scanlan DJ, Ostrowski M, Mazard S, Dufresne A, Garczarek L, Hess WR et al. (2009). Ecological genomics of marine picocyanobacteria. *Microbiol Mol Biol Rev* **73**: 249–299.
- Scott KM, Henn-Sax M, Harmer TL, Longo DL, Frame CH, Cavanaugh CM. (2007). Kinetic isotope effect and biochemical characterization of form IA RubisCO from the marine cyanobacterium *Prochlorococcus marinus* MIT9313. *Limnol Oceanogr* **52**: 2199–2204.
- Shi D, Xu Y, Morel FMM. (2009). Effects of the pH/pCO₂ control method on medium chemistry and phytoplankton growth. *Biogeosciences* **6**: 1199–1207.
- Shibata M, Katoh H, Sonoda M, Ohkawa H, Shimoyama M, Fukuzawa H et al. (2002). Genes essential to sodium-dependent bicarbonate transport in cyanobacteria. *J Biol Chem* **277**: 18658–18664.
- Steglich C, Futschik M, Rector T, Steen R, Chisholm SW. (2006). Genome-wide analysis of light sensing in *Prochlorococcus*. *J Bacteriol* **188**: 7796–7806.
- Steglich C, Futschik ME, Lindell D, Voss B, Chisholm SW, Hess WR. (2008). The challenge of regulation in a minimal photoautotroph: Non-coding RNAs in *Prochlorococcus*. *PLoS Genet* **4**: e1000173.
- Suárez-Fariñas M, Pellegrino M, Wittkowski KM, Magnasco MO. (2005). Harshlight: a "corrective make-up" program for microarray chips. *BMC Bioinform* **6**: 294.
- Thompson AW, Huang K, Saito MA, Chisholm SW. (2011). Transcriptome response of high- and low-light-adapted *Prochlorococcus* strains to changing iron availability. *ISME J* **5**: 1580–1594.
- Tolonen AC, Aach J, Lindell D, Johnson ZI, Rector T, Steen R et al. (2006). Global gene expression of *Prochlorococcus* ecotypes in response to changes in nitrogen availability. *Mol Syst Biol* **2**: 53.
- Van Mooy BAS, Rocap G, Fredricks HF, Evans CT, Devol AH. (2006). Sulfolipids dramatically decrease phosphorus demand by picocyanobacteria in oligotrophic marine environments. *Proc Natl Acad Sci USA* **103**: 8607–8612.
- Van Mooy BAS, Fredricks HF, Pedler BE, Dyhrman ST, Karl DM, Koblížek M et al. (2009). Phytoplankton in the ocean use non-phosphorus lipids in response to phosphorus scarcity. *Nature* **458**: 69–72.
- Vaultot D, Marie D, Olson RJ, Chisholm SW. (1995). Growth of *Prochlorococcus*, a photosynthetic prokaryote, in the equatorial Pacific Ocean. *Science* **268**: 1480–1482.

Wakabayashi K, Misawa Y, Mochiji S, Kamiya R. (2011). Reduction-oxidation poise regulates the sign of phototaxis in *Chlamydomonas reinhardtii*. *Proc Natl Acad Sci USA* **108**: 11280–11284.

Yao D, Kieselbach T, Komenda J, Promnares K, Hernández Prieto MA, Tichy M et al. (2007). Localization of the small CAB-like proteins in photosystem II. *J Biol Chem* **282**: 267–276.

Zinser ER, Johnson ZI, Coe A, Karaca E, Veneziano D, Chisholm SW. (2007). Influence of light and temperature on *Prochlorococcus* ecotype distributions in the Atlantic Ocean. *Limnol Oceanogr* **52**: 2205–2220.

Zinser ER, Lindell D, Johnson ZI, Futschik ME, Steglich C, Coleman ML et al. (2009). Choreography of the transcriptome, photophysiology, and cell cycle of a minimal photoautotroph, *Prochlorococcus*. *PLoS One* **4**: e5135.

Supplementary Information accompanies this paper on The ISME Journal website (<http://www.nature.com/ismej>)